A Passive Micromixer for Bioanalytical Applications

Ioanna N. KEFALA, Vasileios E. PAPADOPOULOS, Georgia KARPOU, George KOKKORIS*, George PAPADAKIS, and Angeliki TSEREPI*

*Corresponding authors: Tel.: ++30 2106503264; Fax: ++30 210 6511723; Email: gkok@imel.demokritos.gr, atserepi@imel.demokritos.gr
Institute of Nanoscience and Nanotechnology, NCSR "Demokritos", Greece

Abstract Three passive micromixers with different geometries, i.e. zigzag, spiral, and split and merge (SaM) with labyrinthine channels, are compared with respect to their mixing efficiency by means of a computational study. The specifications are imposed from flexible printed circuit (FPC) technology which is used for their fabrication and from the applications to be implemented, i.e. the mixing of biochemical reagents. The computations include the numerical solution of continuity, Navier-Stokes, and mass conservation equations in 3d by ANSYS Fluent. The highest mixing efficiency is calculated for the SaM micromixer with the labyrinthine channel. Compared to a linear micromixer, the spiral micromixer improves the mixing efficiency by 8%, the zigzag by 11%, and the SaM by 92%; the diffusion coefficient of the biomolecule is 10^{-10} m^2/s, the Reynolds number is 0.5, and the volume of each micromixer is 2.54 μl. The best of the three designs is realized by FPC technology and is experimentally evaluated by fluorescence microscopy.

Keywords: Passive Micromixer, Microflow, split and recombine, Lab-on-a-Chip, LoC, FPC technology, Dean Vortices

1. Introduction

The vision of integrating several functions of a (bio)chemical analysis laboratory on a chip drives the research, design, and development of microfluidic devices. Microfluidic devices play an important role in various applications; transport, mixing, separation, and/or reactions, functions necessary for the so called Lab-on-a-Chip (LoC) systems. Usually, their operation defines the total performance of LoC systems; A well-designed micromixer, for instance, can reduce the analysis time and the footprint of a LoC system (Ottino and Wiggins, 2004).

Generally, the objective of a micromixer is the rapid mixing between two liquid flows. However, due to the small dimensions of the channels of the micromixer, such flows are usually governed by low Reynolds (Re) numbers: Turbulence is absent and hence mixing is slow.

Micromixers can be classified into two categories: Active and passive ones (Lee et al., 2011; Mansur et al., 2008). Passive are the micromixers which do not require external energy (besides the energy required for the pumping of the fluid) as opposed to active which use the disturbance generated by an external field for the mixing process. Even though the active micromixers are more effective than the passive ones (Alam and Kim, 2012; Fu and Lin, 2007; Mansur et al., 2008), they entail more complex and expensive fabrication processes, and their integration with other micro-components is more difficult. In addition, active micromixers have higher cost for active control, compared to the passive ones, and typically higher power consumption. Furthermore, some active mixing mechanisms such as ultrasonic waves or high temperature gradients can damage biological samples making them unsuitable for the analysis process (Capretto et al., 2011; Nguyen et al., 2008).

Several designs of passive micromixers have been proposed in the literature such as Y- or T-shaped and multi-inlet channels with

parallel or serial lamination (Gobby et al., 2001; Hessel et al., 2003). The multi-lamination increases the mixing efficiency by decreasing the mixing path and increasing the interface area between the mixing streams.

Other designs focus on creating flow perturbation by barriers (posts) (Bhagat et al., 2007; Jeon and Shin, 2009) or grooves (Kee and Gavriilidis, 2008; Stroock et al., 2002) or by using channels with a suitably varying cross section (Wang et al., 2012). Based on the same principle, designs with zigzag channels (Jeon and Shin, 2009), helical flow patterns, expansion units (Sudarsan and Ugaz, 2006), logarithmic spirals (Scherr et al., 2012) and split and merge (or recombine) geometries (Bhopte et al., 2010) or even complex 3d geometries (Viktorov and Nimafar, 2013) have been also proposed.

The motivation of this work is the design of a planar passive micromixer for biochemical applications, such as the enzymatic digestion of DNA. Taking the example of DNA digestion, an effective digestion process requires an effective/rapid mixing of the enzyme with the DNA. However, the enzymes, and generally the biomolecules, have very low diffusion coefficient, varying from 10^{-9} to 10^{-11} m^2/s (Ottino and Wiggins, 2004), which makes the design of a rapid micromixer a challenging problem. The study in this work and the scope of the applications of the proposed passive micromixer cover mixing processes in biomolecule solutions.

In a previous work (Papadopoulos et al., 2014), a three inlet zigzag micromixer was utilized for the enzymatic digestion of DNA. The required length for complete mixing was estimated by numerical calculations. Here, the work is extended to three different designs of passive micromixers, a zigzag, a spiral, and a split and merge micromixer with labyrinthine channel (SaM-labyrinth), compared in a computational study, aiming to the selection of the most efficient design. A linear channel micromixer is also simulated as a comparison baseline. All micromixers have two inlets and their specifications (channel shape and dimensions) are imposed from the flexible printed circuit (FPC) technology (Papadopoulos et al., 2014) implemented for their fabrication.

The rest of the paper is structured as follows: In Sec. 2, the mathematical model is presented. In Sec. 3, the designs and simulation results are described. In Sec. 4, the fabrication process is described and realized devices are shown. The experimental evaluation by fluorescence microscopy is described in Sec. 5. The last section includes the conclusions.

2. Mathematical model

The model consists of the continuity equation

$$\nabla \cdot \mathbf{u} = 0 \tag{1}$$

and the Navier-Stokes equation

$$\rho \mathbf{u} \cdot \nabla \mathbf{u} = -\nabla p + \mu \nabla^2 \mathbf{u} \tag{2}$$

where $\mathbf{u}$ is the vector of fluid velocity, ρ, μ and p are the density, dynamic viscosity, and pressure of the fluid. The model includes also the mass conservation equation of the solute (the enzyme in a DNA digestion process)

$$\nabla \cdot \left(-D \nabla C\right) + \mathbf{u} \cdot \nabla C = 0 \tag{3}$$

where C and D are the concentration and diffusion coefficient of the solute in the solution. No slip condition for the velocity and zero derivatives for the concentration are considered at the walls of the micromixer. Fully developed parabolic profiles of velocity are considered at the inlets, whereas zero derivatives of both velocity and concentration in the outflow direction are considered at the outlet; the micromixer has two inlets and one outlet.

The density and the dynamic viscosity of the solution are those of water at 20 ^{o}C. The equations are solved in 3d by the finite volume method with ANSYS Fluent (ANSYS, Inc., Canonsburg, PA).

The performance of the micromixer is evaluated by the mixing efficiency, *n*, (Nguyen, 2008) at a vertical-to-flow cross section

$$n = 1 - \sqrt{\frac{1}{N}\sum_{i=1}^{N}\left(\frac{C_i - \bar{C}}{\bar{C}}\right)^2} \qquad (4)$$

$\bar{C}$ is the expected concentration of the solute at full mixing and C_i is the local concentration at point *i* of the cross section. *N* is the number of points in the cross section.

3. Designs and simulation results

3.1 Proposed designs and evaluation conditions

The micromixer specifications regarding the channel dimensions stem from the fabrication technology (see Section 4). The height of the channel is 60 μm, equal to the thickness of the photo-imageable dry film (Papadopoulos et al., 2014) where the channel will be formed. The minimum width of the channels is 150 μm, appropriate for a reproducible lithographic process. All designs have two inlets with channel width equal to 150 μm, merging in a 300 μm-wide main channel. The total volume of each micromixer is 2.54 μl. The micromixers are evaluated under the same flow conditions: The mean velocity at both inlets is set at 5 mm/s corresponding to a volumetric flow rate of 2.7 μl/min, i.e. a total rate of 5.4 μl/min at the outlet. The Re number under these conditions is equal to 0.5.

In Fig. 1, the designs (or the lithographic masks) of the micromixers are presented. The first design (Fig. 1a) is a composition of two spirals with two turns joined at the center of the micromixer with two mirrored semicircles. The centrifugal forces of this design will create flow stretching and desirably, depending on the flow conditions, a secondary flow due to the so-called Dean vortices (Schönfeld and Hardt, 2004). The second design (Fig. 1b) is a zigzag geometry with a 60^o angle and a total length of 87.7 mm. Zigzag geometries create, along with Dean vortices, continuous sudden changes of the flow direction, thus improving the mixing. The flow stretching and the secondary flow are combined with splitting and merging of the flow in the last design (Fig. 1c): The SaM-labyrinth consists of concentric rings where the flow is splitting and merging while moving from the outer channels to the inner ones.

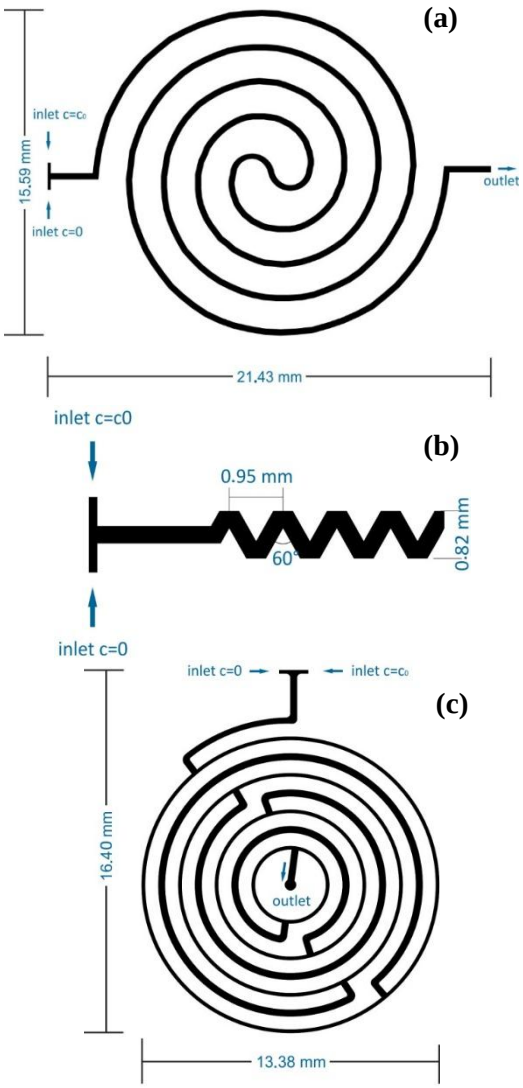

Fig. 1 Top – down view (or lithographic mask) of the micromixer with a) spiral geometry, b) zigzag geometry (only a part is shown), c) SaM – labyrinth geometry

3.2 Simulation results and discussion

For the numerical solution, meshes with hexahedral elements are built for all geometries. For mesh independent solutions, approximately 25 millions of elements are required for the spiral, the zigzag and SaM-

labyrinth, and almost 16 millions of elements are required for the linear micromixer. The procedure for the mesh independency of the solution involves the continuous doubling of the elements until the solution (velocity and concentration) shows small difference with the previous one; in particular, the densification of the mesh stopped when the difference of the mixing efficiency between successive solutions was less than 2.5%.

The calculated mixing efficiencies at the outlet of the micromixers are shown in Fig. 2; the SaM-labyrinth micromixer provides faster mixing than the other two designs. Compared to the linear micromixer, the spiral improves mixing by 8%, the zigzag by 11% and the SaM-labyrinth by 92%.

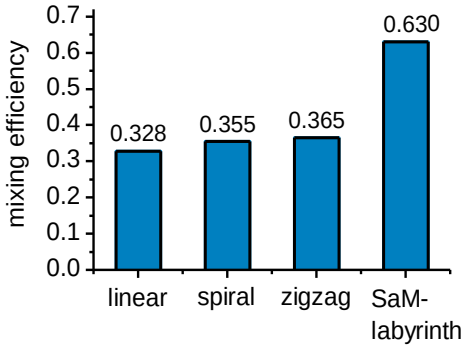

Fig. 2 Comparison of micromixers in terms of mixing efficiency [Eq. (4)] at the outlet (diffusion coefficient of the biomolecule is 10^{-10} m^2/s)

Fig. 3 shows the concentration contours at the middle height of the SaM-labyrinth micromixer and Fig. 4 shows the profiles of concentration at the flow-stream merging areas (junctions) of the same micromixer. It is seen that in all four merging areas, high concentration gradients occur, a feature which enhances mixing.

Three mechanisms potentially improve the mixing efficiency of the SaM–labyrinth micromixer: The formation of Dean vortices due to the curved channels, the decrease of the mixing length by splitting the flow-stream, and the induction of a concentration gradient at the junctions. Regarding the last, the geometry of the SaM-labyrinth induces a greater concentration gradient at the junctions compared to the normal split and merge case. For example, as shown in Fig. 4, the concentration difference at junction (A) is ca. 1 while for the normal split and merge case this difference would have been ca. 0.6 (0.8-0.2).

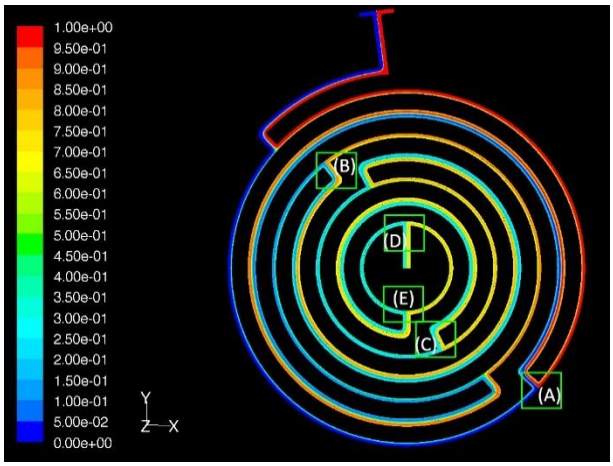

Fig. 3 Concentration contours at the middle height of the SaM-labyrinth micromixer. Regions (A) - (D) are the merging areas from the second (the first is out of the labyrinth) to the last junction, respectively; the concentration profiles at these regions are shown in Fig. 4.

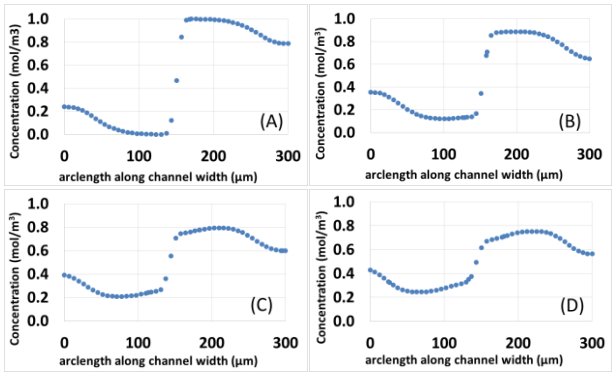

Fig. 4 Concentration profiles at the four merging areas [(A)-(D)] of the SaM-labyrinth micromixer shown in Fig. 3. Each merging creates high concentration gradients at the junction.

The results of Fig. 2 also show that the mixing efficiency of the spiral and zigzag micromixer are close to the linear micromixer. The reason for the smaller than expected increase of the mixing efficiency is the low Dean number (K) ranging from 0.06 to 0.23. K quantifies the Dean vortices (secondary flow), (Schönfeld and Hardt, 2004) and is formulated as

$$K = \mathrm{Re}\sqrt{\frac{D_h}{R_c}} \qquad (5)$$

where D_h is the hydraulic diameter of the channel, and R_c is the radius of curvature of the curved microchannel.

Indeed, an increase of the flow velocity, e.g. by increasing the volumetric flow rate, or/and an increase of D_h, e.g. by increasing the depth of the channel (this would require the use of a thicker film for the fabrication of the channel), would increase K and hence the mixing efficiency of all micromixers. In this case, the difference of the mixing efficiency between the linear and the zigzag (spiral) micromixers is expected to be greater than the calculated 8%.

4. Micromixer fabrication

The structural materials for the micromixer are a commercially available printed circuit board (PCB) which is used as substrate and a photo-imageable polyimide(PI)-based dry film (Dupont®, PC1000 series) where the channels of the micromixer are formed. These materials are chosen for their excellent functional characteristics, their compatibility to mass production, and their capability to form integrated devices.

In our process, the PI-based film acts as a negative photoresist for the formation of the micromixer channel.

The process flow is shown in Fig. 5. The fabrication of the micromixers starts with the lamination of the PI-based film on the PCB substrate using a roll laminator operating at atmospheric pressure at a temperature of 85^{o}C. Subsequently, the substrate is pre-baked at 120^{o}C (to enable the elimination of excess solvent from the film) and UV exposed for 25 s, to form the bottom layer of the microfluidic network. Following, the substrate is hard-baked at 160^{o}C for 2 hours in an oven. On top of that, a second photo-imageable PI-based dry film is laminated under the same conditions, (pre-baked, UV exposed, developed in a 1% w/w aqueous sodium bicarbonate solution (Na_2CO_3) and hard baked as previously described) so as to pattern the microfluidic channel. To allow injection of fluid samples, holes are drilled for the flow inlet and outlet using a pedestal drill.

Finally, the microfluidic network is sealed by means of a laminated polyolefin film (StarSeal Advanced Polyolefin Film, STARLAB International GmbH) to form enclosed microchannels; the polyolefin film is suitable for optical detection due to its high transparency and low auto-fluorescence.

An image of the fabricated SaM micromixer is shown in Fig. 6.

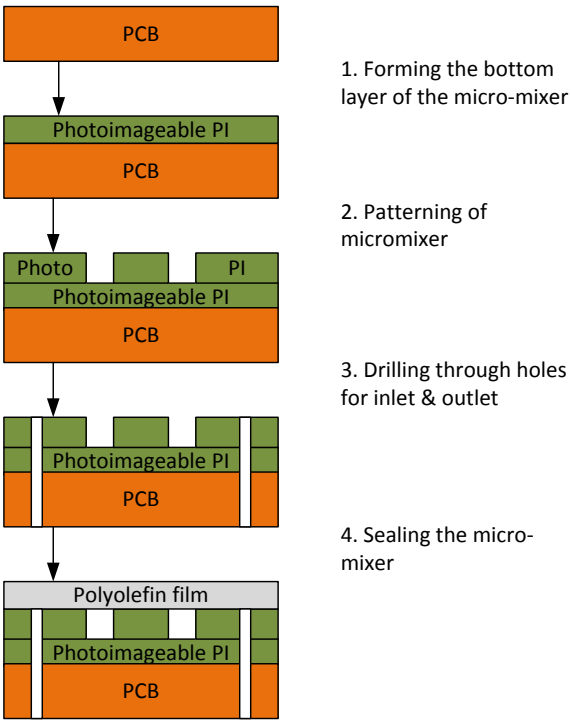

Fig. 5 Process flow of fabrication of the micromixer

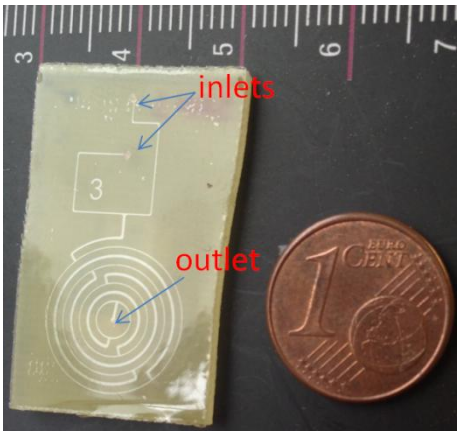

Fig. 6 Fabricated SaM-labyrinth micromixer

5. Experimental evaluation of the micromixer

The SaM-labyrinth micromixer is experimentally validated by means of fluorescence microscopy. A fluorescence microscope (Axioscope 2 Plus epifluorescence microscope by Carl Zeiss, Germany) equipped with a Micropublisher 3.3 RTV (Qimaging) digital camera is used. The objective is 10×/0.3.

The two solutions used to evaluate the efficiency of the micromixer are distilled water (dH_2O) and an aqueous solution of 3×10^{-5} M fluorescein. The diffusion coefficient of fluorescein in water is 4.9×10^{-10} m^2/s (Li et al., 2012), i.e. in the range of values for biomolecules.

To perform the evaluation tests, fluidic interfaces are necessary. In particular, a plexiglass, custom-made chip holder fabricated in-house to be compatible with commercially available Upchurch® Nanoport fittings, is used. The two solutions are injected in the inlets with a volumetric flow rate of 2.7 μl/min each by means of a syringe pump (Chemyx Inc, Fusion 200).

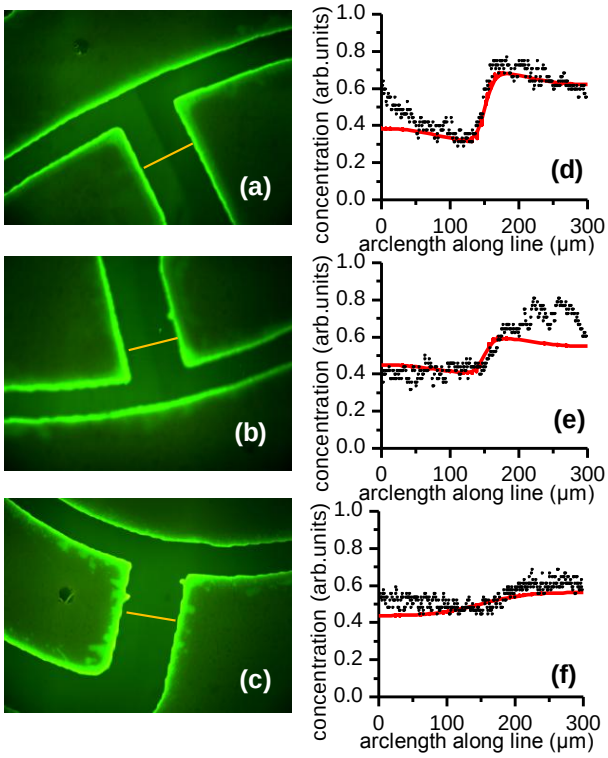

Fig. 7 Images at junctions a) B (Fig. 3) and b) C (Fig. 3) as well as at c) the last split (region E in Fig. 3) of the SaM-labyrinth micromixer. The normalized fluorescence intensity (points) along the lines drawn in Figs. 7(a-c-) are shown in Figs. 7 (d-f). In the latter, simulation results (solid curves) along the same lines are shown; the diffusion coefficient is 4.9×10^{-10} m^2/s.

A band-pass excitation filter at 485 nm and a band-pass emission filter at 534 nm are used for the visualization. The software used for the image capture is ImagePro Plus (Media Cybernetics, Inc., USA).

Images at the third and fourth junctions [see noted areas (B) and (C) in Fig. 3] as well as at the last split are shown in Figs. 7a-c. The normalized fluorescence intensity values along the lines shown in Figs. 7a-c are depicted in Figs. 7d-f. In the latter, simulation results along the same lines are shown. The diffusion coefficient in this case is that of fluorescein, i.e. 4.9×10^{-10} m^2/s, and not 10^{-10} m^2/s as in the results presented in Sec. 3. Despite the noise in the experiments, the measurements are consistent with the simulation results.

6. Conclusions

Aiming to the design and realization of a passive micromixer for biochemical applications, a zig-zag, a spiral, and a SaM micromixer with labyrinthine channel are compared through numerical calculations. The comparison is performed under the same conditions and it is based on the specifications imposed by the FPC technology which is used for the fabrication of the micromixers.

For a diffusion coefficient equal to 10^{-10} m^2/s (typical for biomolecules), for Re number equal to 0.5, and for a total volume of 2.54 μl, the mixing efficiency of the SaM-labyrinth is 0.630, whereas it is 0.365 and 0.355 for the zigzag and the spiral micromixers, respectively.

The mixing performance of the SaM-labyrinth micromixer is enhanced by the greater concentration gradient at the junctions (merging areas) compared to the split and merge case. Due to the low Re number (0.5), the Dean number is low for the zigzag and spiral geometries. As a consequence, their

mixing efficiency is close to that of the linear micromixer.

The proposed SaM-labyrinth micromixer is realized with FPC technology on a PCB substrate: The channels of the micromixer are formed on photo-imageable PI-based dry film. It is amenable to mass production, and can be used in microanalytical platforms in combination with other microfluidic devices.

Finally, first results of an experimental evaluation of the SaM-labyrinth micromixer by means of fluorescence microscopy are presented. In particular, mixing of distilled water and an aqueous solution of fluorescein is performed in the micromixer. The fluorescence intensity measurements compares well with the simulation results.

Future work refers to the application of the SaM-labyrinth micromixer to DNA digestion process as well as its integration to a microanalytical platform.

Acknowledgements

This work was supported by the project “DoW-DNA on Waves: An integrated diagnostic system" (LS7-276, program "Supporting post-doctoral researchers", Ministry of Education, Lifelong Learning, and Religious Affairs); the source of funding is the European Social Fund (ESF) -European Union and National Resources.

The fluorescence experiments were performed at the Immunoassays and Immunosensors Laboratory of the Institute of Nuclear & Radiological Sciences & Technology, Energy & Safety of NCSR “Demokritos”; the authors would like to thank Drs P. S. Petrou and S. E. Kakabakos for their guidance on fluorescence measurements. The authors would like to thank Dr D. Moschou for useful discussions, and D. Papageorgiou for his help on the fabrication of the chip-holder.

References

Alam, A., Kim, K.-Y., 2012. Analysis of mixing in a curved microchannel with rectangular grooves. Chemical Engineering Journal 181–182, 708-716.

Bhagat, A.A.S., Peterson, E.T., Papautsky, I., 2007. A passive planar micromixer with obstructions for mixing at low Reynolds numbers. Journal of Micromechanics and Microengineering 17, 1017.

Bhopte, S., Sammakia, B., Murray, B., 2010. Numerical study of a novel passive micromixer design, Thermal and Thermomechanical Phenomena in Electronic Systems (ITherm), 2010 12th IEEE Intersociety Conference on, pp. 1-10.

Capretto, L., Cheng, W., Hill, M., Zhang, X., 2011. Micromixing Within Microfluidic Devices, in: Lin, B. (Ed.), Microfluidics. Springer Berlin Heidelberg, pp. 27-68.

Fu, L.-M., Lin, C.-H., 2007. A rapid DNA digestion system. Biomed Microdevices 9, 277-286.

Gobby, D., Angeli, P., Gavriilidis, A., 2001. Mixing characteristics of T-type microfluidic mixers. Journal of Micromechanics and Microengineering 11, 126.

Hessel, V., Hardt, S., Löwe, H., Schönfeld, F., 2003. Laminar mixing in different interdigital micromixers: I. Experimental characterization. AIChE Journal 49, 566-577.

Jeon, W., Shin, C.B., 2009. Design and simulation of passive mixing in microfluidic systems with geometric variations. Chemical Engineering Journal 152, 575-582.

Kee, S.P., Gavriilidis, A., 2008. Design and characterisation of the staggered herringbone mixer. Chemical Engineering Journal 142, 109-121.

Lee, C.-Y., Chang, C.-L., Wang, Y.-N., Fu, L.-M., 2011. Microfluidic Mixing: A Review. International Journal of Molecular Sciences 12, 3263-3287.

Li, Y., Zhang, D., Feng, X., Xu, Y., Liu, B.F., 2012. A microsecond microfluidic mixer for characterizing fast biochemical reactions. Talanta 88, 175-180.

Mansur, E.A., Ye, M., Wang, Y., Dai, Y., 2008. A State-of-the-Art Review of Mixing in Microfluidic Mixers. Chinese Journal of Chemical Engineering 16, 503-516.

Nguyen, N.-T., 2008. Micromixers

fundamentals, design and fabrication. Elsevier.
Nguyen, T.N.T., Kim, M.-C., Park, J.-S., Lee, N.E., 2008. An effective passive microfluidic mixer utilizing chaotic advection. Sensors and Actuators B: Chemical 132, 172-181.
Ottino, J.M., Wiggins, S., 2004. Introduction: mixing in microfluidics. Philosophical Transactions of the Royal Society of London. Series A: Mathematical, Physical and Engineering Sciences 362, 923-935.
Papadopoulos, V., Kefala, I., Kaprou, G., Kokkoris, G., Moschou, D., Papadakis, G., Gizeli, E., Tserepi, A., 2014. A passive micromixer for enzymatic digestion of DNA. Microelectronic Engineering 124, 42–46.
Scherr, T., Quitadamo, C., Tesvich, P., Park, D.S.W., Tiersch, T., Hayes, D., Choi, J.W., Nandakumar, K., Monroe, W.T., 2012. A planar microfluidic mixer based on logarithmic spirals. Journal Of Micromechanics And Microengineering 22, 055019.
Schönfeld, F., Hardt, S., 2004. Simulation of helical flows in microchannels. AIChE Journal 50, 771-778.
Stroock, A.D., Dertinger, S.K.W., Ajdari, A., Mezić, I., Stone, H.A., Whitesides, G.M., 2002. Chaotic Mixer for Microchannels. Science (New York, N.Y.) 295, 647-651.
Sudarsan, A.P., Ugaz, V.M., 2006. Fluid mixing in planar spiral microchannels. Lab on a Chip 6, 74-82.
Viktorov, V., Nimafar, M., 2013. A novel generation of 3D SAR-based passive micromixer: efficient mixing and low pressure drop at a low Reynolds number. Journal of Micromechanics and Microengineering 23, 055023.
Wang, L., Liu, D., Wang, X., Han, X., 2012. Mixing enhancement of novel passive microfluidic mixers with cylindrical grooves. Chemical Engineering Science 81, 157-163.